

# Detection of 3D salient points in magnetic resonance images using the dual-tree complex wavelet transform

Nicole Z. Kovacs  
Departamento de Computação  
Universidade Federal de São Carlos  
São Carlos - SP  
Email: 558419@comp.ufscar.br

Ricardo J. Ferrari  
Departamento de Computação  
Universidade Federal de São Carlos  
São Carlos - SP  
Email: rferrari@dc.ufscar.br

**Abstract**—Detection of 3D salient points in medical images has many important applications such as image registration and mesh positioning for the purpose of segmentation of important anatomical structures. In this study, we present preliminary results of a proposed method for the detection of 3D salient points in Magnetic Resonance (MR) images of human brain. Our method, which is based on the Dual-Tree Complex Wavelet Transform, combines the oriented wavelet sub-bands (by multiplying the ones on the same scale and upsampling the result to an upper level scale) to create an image map in which local maxima correspond to the salient points. Qualitative assessment was conducted using 566 brain MRI images, whose results were combined together to create a point cloud showing the concentration of the salient points on important brain regions. The results indicate that our method has a great potential to detect important 3D salient points in MR images.

## I. INTRODUCTION

Magnetic resonance imaging (MRI) has become a core resource for studying and diagnosing various diseases and syndromes of the central nervous system. In these cases, it is often necessary to segment and measure the volume of important brain structures in order to aid both diagnosis and follow up of the disease's evolution.

Salient points are used in several image processing and computer vision applications, such as object recognition [2], orientation of certain transformations, and as a way to represent images in database indexing [14]. Among medical images, 3D salient points are also used to guide the registration of different image modalities [7] (MRI and Computerized Tomography, for example), to construct probabilistic anatomic atlases [1], and to facilitate the positioning of mesh models in 3D images [5].

The techniques presented in the image processing literature for detecting 3D salient points use different approaches, going from the use of first-order differential operators to identify corners [6] to the adjustment of parametric models and application of learning based methods [11], [15]. In our research group, the technique currently used for detecting 3D salient points in Magnetic Resonance (MR) images is based on the Phase Congruency (PC).

In this paper, we propose to use the Dual-Tree Complex Wavelet Transform (DT-CWT) as an alternative method to replace the PC-based technique, since it has better computational efficiency (less time and space complexity) due to the dual-tree implementation and generates complex coefficients whose values of magnitude and phase directly relate to the quality and localization of important attributes of an image, such as edges and corners.

This manuscript is organized as follows: Section II describes the methodology used for the development of the proposed method, followed by preliminary results and discussions in Section III and final conclusions in Section IV.

## II. MATERIALS AND METHODS

Fig. 1 illustrates a block diagram of the proposed method. Further details of each block are presented in this section as follows.

### A. Preprocessing

All images used in this study were preprocessed to reduce noise and bias field using, respectively, the Non-Local Means [3] and the N4-ITK [13] techniques, and for brain extraction, using the Robust Brain Extraction (ROBEX) [8] technique. In addition, affine image registration was applied to all images in the database.

### B. 3D Dual-Tree Complex Wavelet Transform

Since its creation in the early 1980's, the Discrete Wavelet Transform (DWT) [10] has been successfully explored in numerous image processing applications because of its accuracy to represent signals with singularities, such as peaks. Despite their success on various digital signal processing applications, the DWT has yet some limitations, such as signal translation variance, aliasing and poor directional selectivity.

The DT-CWT was introduced by Kingsbury [9] as an improvement over the DWT that overcomes its previously mentioned limitations. In order to do so, the DT-CWT uses two mother wavelets ( $\psi_h(x)$  and  $\psi_g(x)$ ), one for each tree, where one is the approximate the Hilbert transform of the other

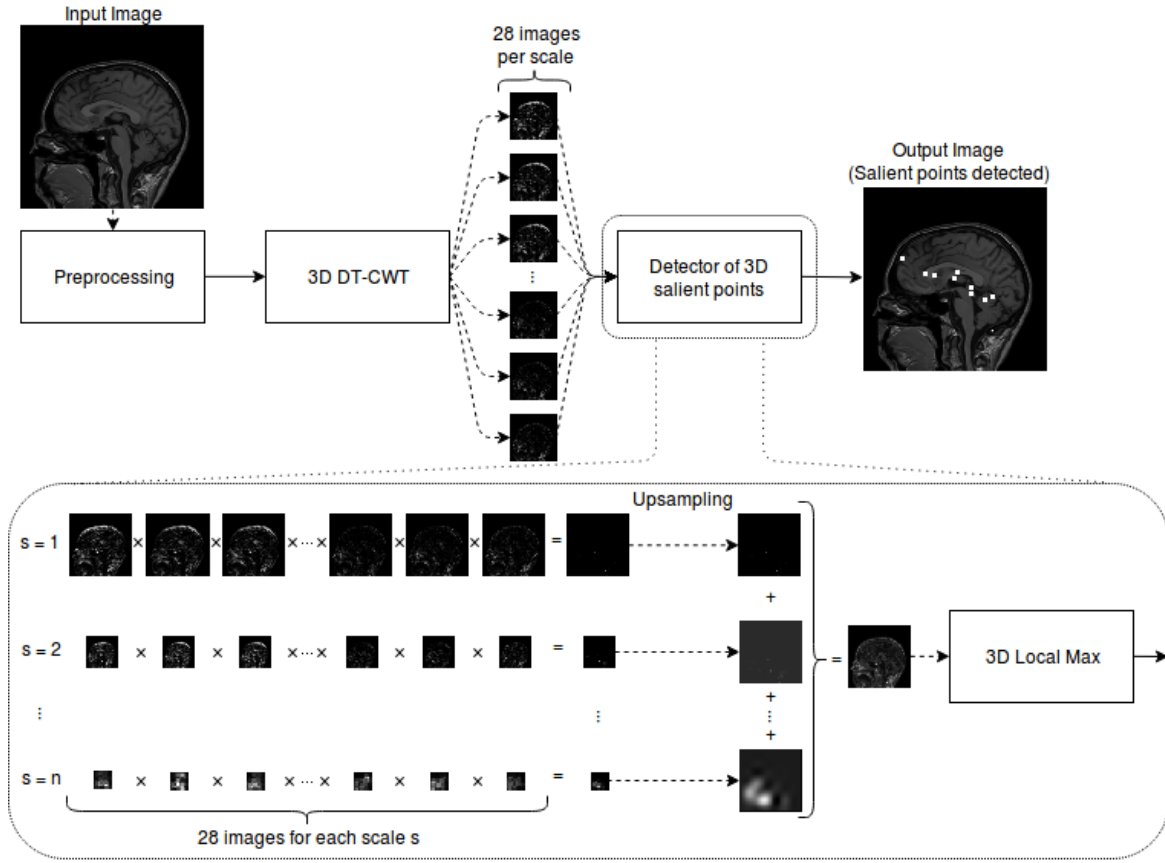


Fig. 1: Block diagram of the proposed method.

( $\psi_g(x) \approx \mathcal{H}\{\psi_h(x)\}$ ). Thus, the analytic complex wavelet transform is defined as

$$\psi(x) = \psi_h(x) + j\psi_g(x), \quad (1)$$

where  $j = \sqrt{-1}$  is the unit imaginary number. This construction, which provides both local magnitude and phase information of a signal, allows that negative frequencies be suppressed and aliasing effects reduced, while still maintaining an approximated invariance of the transform regarding its signal translation.

As described in [12], the DT-CWT can be extended to three dimensions by separating the signal filtering among the three axes and using the same process of uni-dimensional signals separately. Thus the 3D DT-CWT is defined as

$$\psi(x, y, z) = \psi(x) \times \psi(y) \times \psi(z). \quad (2)$$

### C. Detector of 3D salient points

The proposed method for the detection of 3D salient points in MR images, illustrated in Fig. 1, is an adaptation from [4], where the salient points are defined as local maximal of an energy map accumulator computed from the combination of the 28 DT-CWT sub-bands from each scale.

In this case, for a given input image with dimensions of  $w \times h \times d$  voxels, the image is decomposed into  $m$  scales ( $s = 1, \dots, m$ ), where each sub-band  $s$  will have a

dimension of  $\frac{w}{2^s} \times \frac{h}{2^s} \times \frac{d}{2^s}$ . As per the DT-CWT orientation decomposition, from each point of each scale, a set  $C_s = \{\rho_1 e^{j\theta_1}, \dots, \rho_{28} e^{j\theta_{28}}\}$  of 28 complex coefficients is obtained. This directional information is useful for elaborating an energy map that can be used for the detection of the salient points, since it allows emphasizing small points, corners and junctions and ignoring borders and uniform areas in the image.

The energy map, which gives a measure of local energy for each voxel, is computed by the product of the 28 sub-band magnitudes  $\rho_i$  resulting from the DT-CWT image decomposition as

$$E(C_s) = \alpha^s \left( \prod_{i=1}^{28} \rho_i \right)^\beta, \quad (3)$$

where  $\alpha$  and  $\beta$  control the relative weight of the sub-bands. By adjusting  $\alpha$  and  $\beta$ , we can emphasize small-scale features but with the drawback of increasing the algorithm's noise sensitivity.

The energy map accumulator,  $A$ , is created by interpolating all resulting energy maps  $E(C_s)$  by a  $2^s$  factor and summing all of them together:

$$A = \sum_{s=1}^m f(E(C_s)), \quad (4)$$

where  $f(\cdot)$  represents the Gaussian interpolation operation applied to the map  $E(C_s)$  from the scale  $s$ . The maximum

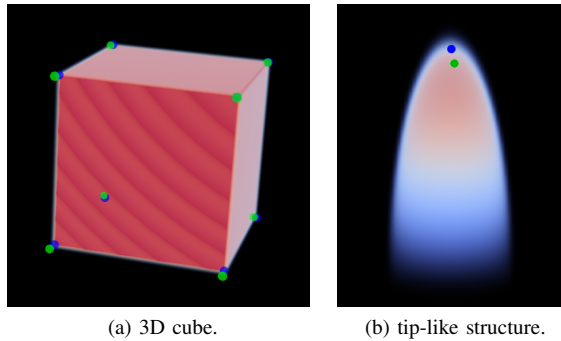


Fig. 2: Results of the proposed method for detection of 3D salient points on synthetic images. Blue and green dots correspond, respectively, to ground-truth points and points automatically detected.

values of the accumulator map represent the detected salient points.

#### D. Image datasets

The images used in this study were obtained from the BrainWeb<sup>1</sup> and the IXI<sup>2</sup> datasets. BrainWeb provides computer simulated images with different degrees of noise and bias field. A few images from this database were used to evaluate the algorithm’s robustness regarding noise and bias field. The IXI dataset is composed of 566 images obtained from three London hospitals: Hammersmith Hospital (HH), Guy’s Hospital (GH), and the Institute of Psychiatry (IoP), where each hospital has their own MRI scanner and acquisition protocol. In this study, the images were preprocessed for noise reduction and bias field correction, and affine-registered to a template image. The IXI dataset was used to evaluate the correctness of the algorithm throughout numerous cases.

### III. PRELIMINARY RESULTS AND DISCUSSIONS

In this section we present and discuss some preliminary results obtained by the method being developed for the detection of 3D salient points in MR images.

#### A. Results using synthetic images

A thoroughly study using parametric model generated images (a 3D cube and a tip-like structure) was conducted in order to evaluate the accuracy of our method in identifying isolated salient points. Experiments were also performed to assess the influence of the  $\alpha$  and  $\beta$  parameters on the final results and to determine the values that provide the best detection accuracy. The study was performed by exhaustively varying the parameters and computing the average distance of the points automatically detected to the ground-truth points, which in the case of a 3D cube are its corners and the tip of the tip-like structure. The best set of parameters was then chosen as the one providing the smallest computed average distance.

Analysis of the influence of the number of scales used in the DT-CWT representation on the detection results was also performed and it was found that at least three scales should be used to avoid large amount of false-positive detections. Fig. 2 illustrates the models used in this experiment and the results obtained using the best set of parameters. It can be noticed that the detected points (green) are very close to the ground-truth points (blue). Despite the simplicity of the synthetic images, the results have confirmed the potential of the proposed method for the detection of 3D salient points.

#### B. MRI results

To test the stability of the proposed 3D salient points detector in MR images, seven important points located at the occipital and frontal horns, and corpus callosum’s genu (see red circles in Fig. 3a) were selected in a noise- and bias-free image from the BrainWeb database. The image was then corrupted by Rician noise (3% and 5%) and two levels of bias field (20% and 40%). The results of our detector of 3D salient points applied to these images are shown in Figs. 3a–3e. Upon observation of Figs. 3b and 3c, it can be noticed that our method is still sensitive to noise, as it does not identify all the salient points in the selected points in the images. Figs. 3d and 3e, on the other hand, illustrate that the method is significantly robust to bias field, since it has correctly detected the same important points regardless of the level of bias field in the image.

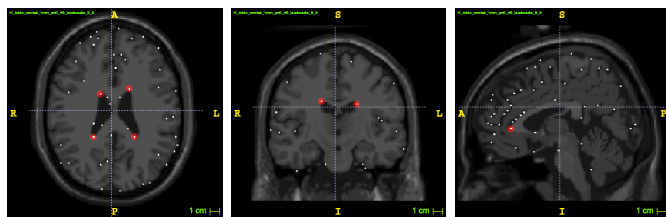
In order to assess the detection consistency in large-scale population, a total of 566 MR images was processed by our method and the results were added together such that salient points, detected throughout most of them, would form point clouds. For better visualization, the resulting sum was convolved with a  $7 \times 7 \times 7$  Gaussian kernel to make the result resemble a probabilistic atlas, as illustrated in red in Fig. 4. In this case, the higher the concentration of salient points is the brighter the red color. As it can be noticed, the concentration of the detected salient points is very high in important anatomical regions of the MR images, such as the ventricular system and parts of the brain stem.

### IV. CONCLUSIONS

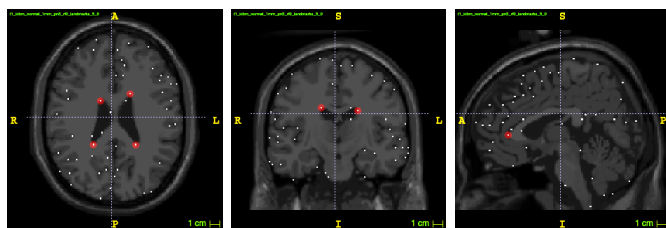
In this ongoing study, we have developed a new method for detecting 3D salient points based on the dual-tree complex wavelet transform. Tests using parametric modeled images were conducted to demonstrate the potential of the proposed method. Moreover, tests with MR images with different levels of noise and bias field were used to study the robustness of the method. In this case, we noticed that our method is considerably robust to bias field but it may require a denoising stage before its application. Finally, primarily tests using clinical MR images showed that our method detects fairly well most of the important salient points in the images, which are located close to important brain structures such as the hippocampus and corpus callosum. Further investigation is still required to quantify the results of the proposed method and,

<sup>1</sup><http://brainweb.bic.mni.mcgill.ca/brainweb/>

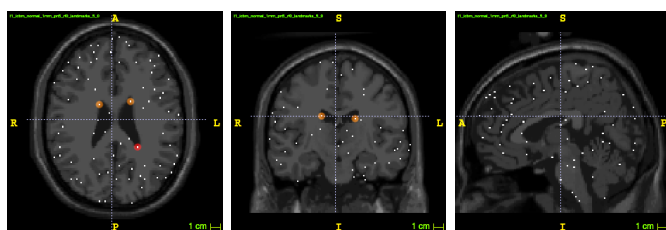
<sup>2</sup><http://brain-development.org/ixi-dataset/>



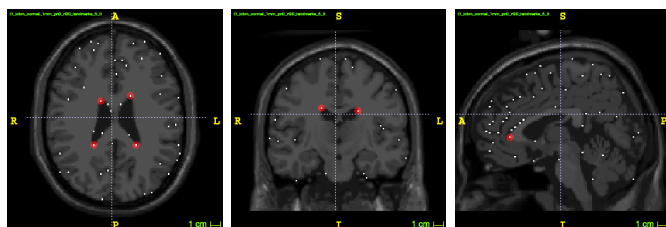
(a) image without any noise or bias field.



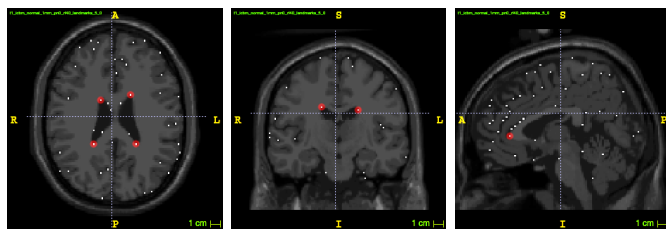
(b) image with 3% of noise and no bias field.



(c) image with 5% of noise and no bias field.



(d) noiseless image with 20% of bias field.



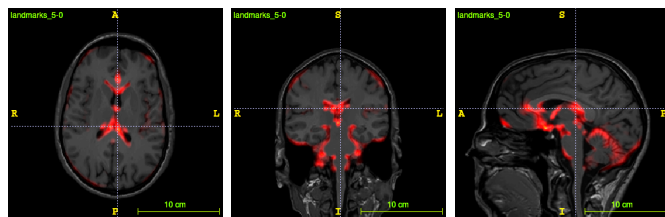
(e) noiseless image with 40% of bias field.

Fig. 3: Influence of noise and bias field on the detection of the salient points. Red circles indicate important locations in the images and orange circles indicate that the detected salient point was detected only closer to the target region.

more importantly, a point descriptor needs to be developed and incorporated to the current method.

#### ACKNOWLEDGMENT

The authors would like to thank the São Paulo Research Foundation (FAPESP) (process number 2015/26512-3) for the



(a) (b) (c)

Fig. 4: Concentration of 3D salient points (illustrated in red) detected in a population of 566 MR images.

financial support given to this research.

#### REFERENCES

- [1] J. Bailleul, S. Ruan, and D. Bloyet, "Automatic atlas-based building of point distribution model for segmentation of anatomical structures from brain MRI," in *Seventh International Symposium on Signal Processing and Its Applications Proceedings*, vol. 2, no. 1-4, 2003, pp. 629–630.
- [2] S. Belongie, J. Malik, and J. Puzicha, "Shape matching and object recognition using shape contexts," *IEEE Transactions on Pattern Analysis and Machine Intelligence*, vol. 24, no. 4, pp. 509–522, 2002.
- [3] A. Buades, B. Coll, and J. M. Morel, "A review of image denoising algorithms, with a new one," *Multiscale Modeling & Simulation*, vol. 4, no. 2, pp. 490–530, 2005.
- [4] J. Fauqueur, N. Kingsbury, and R. Anderson, "Multiscale keypoint detection using the dual-tree complex wavelet transform," Atlanta, GA, USA, Oct 2006, pp. 1625–1628.
- [5] R. J. Ferrari, S. Allaire, A. Hope, J. Kim, D. Jaffray, and V. Pekar, "Detection of point landmarks in 3D medical images via phase congruency model," *Journal of the Brazilian Computer Society*, vol. 17, no. 2, pp. 117–132, 2011.
- [6] W. Förstner and E. Gülch, "A fast operator for detection and precise location of distinct points, corners and centres of circular features," in *Proceedings of the ISPRS Intercommission Workshop*, Interlaken, Switzerland, Jun 1987, pp. 149–155.
- [7] D. Han, Y. Gao, G. Wu, P. T. Yap, and D. Shen, "Robust anatomical landmark detection for MR brain image registration," *Medical Image Computing and Computer-Assisted Intervention (MICCAI)*, vol. 17, no. 1, pp. 186–193, 2014.
- [8] J. E. Iglesias, C. Y. Liu, P. M. Thompson, and Z. Tu, "Robust brain extraction across datasets and comparison with publicly available methods," *IEEE Transactions on Medical Imaging*, vol. 30, no. 9, pp. 1617–1634, 2011.
- [9] N. G. Kingsbury, "The dual-tree complex wavelet transform: a new technique for shift invariance and directional filters," in *Proceedings of the 8th IEEE Digital Signal Processing Workshop*, Bryce Canyon, Utah, USA, Aug 1998, pp. 86–89.
- [10] S. Mallat, "A theory for multiresolution signal decomposition: The wavelet representation," *IEEE Transactions on Pattern Analysis and Machine Intelligence*, vol. 11, no. 7, pp. 674–693, 1989.
- [11] E. Rosten, R. Porter, and T. Drummond, "Faster and better: A machine learning approach to corner detection," *IEEE Transactions on Pattern Analysis and Machine Intelligence*, vol. 32, no. 1, pp. 105–119, 2010.
- [12] I. W. Selesnick and K. Y. Li, "Video denoising using 2d and 3d dual-tree complex wavelet transforms," vol. 5207, San Diego, CA, USA, Aug 2003, pp. 607–618.
- [13] N. J. Tustison, B. B. Avants, P. A. Cook, Y. Zheng, A. Egan, P. A. Yushkevich, and J. C. Gee, "N4ITK: Improved N3 bias correction," *IEEE Transactions on Medical Imaging*, vol. 29, no. 6, pp. 1310–1320, 2010.
- [14] T. Tuytelaars and K. Mikolajczyk, "Local invariant feature detectors: A survey," *Foundations and Trends in Computer Graphics and Vision*, vol. 3, no. 3, pp. 177–280, Jul 2008.
- [15] Y. Zheng, B. Georgescu, and D. Comaniciu, "Marginal space learning for efficient detection of 2D/3D anatomical structures in medical images," in *Proceedings of the Information Processing in Medical Imaging Conference*, vol. 21, Williamsburg, VA, USA, Jun 2009, pp. 411–422.